

Density Functional Theory Study of the Adsorption and Desulfurization of Thiophene and Its Hydrogenated Derivatives on Pt(111): Implication for the Mechanism of Hydrodesulfurization over Noble Metal Catalysts

Houyu Zhu,[†] Wenyue Guo,^{*,†} Ming Li,[†] Lianming Zhao,[†] Shaoren Li,[†] Yang Li,[†] Xiaoqing Lu,[§] and Honghong Shan^{*,†}

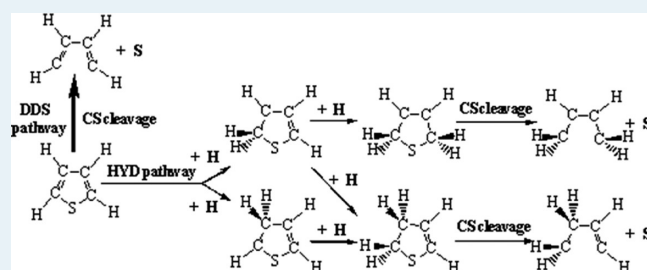
[†]College of Science, [‡]State Key Laboratory for Heavy Oil Processing, China University of Petroleum Qingdao, Shandong 266555, PR China

[§]Department of Physics and Materials Science, City University of Hong Kong, Hong Kong SAR, People's Republic of China

S Supporting Information

ABSTRACT: Desulfurization of thiophene and its hydrogenated derivatives on Pt(111) are studied using self-consistent periodic density functional theory (DFT), and the hydrodesulfurization network is mapped out. On Pt(111), thiophene has two types of adsorption configurations (parallel cross-bridge and partially tilted bridge-hollow), and for its hydrogenated derivatives, the molecule is gradually lifted up from the surface with the addition of hydrogen atoms. In all the adsorbed thiophenic compounds, the S atom is always sp^3 hybridized; the C atom in the methylene group is always sp^3 hybridized, whereas it is either sp^2 or sp^3 hybridized in the methyne group, depending on how the group interacts with the surface Pt atoms. On the basis of the thermodynamic and kinetic analysis of the elementary steps, a direct desulfurization pathway is proposed for the hydrodesulfurization of thiophene on Pt(111). In contrast to the common thought that hydrogenation toward aromatic organosulfur compounds would make desulfurization easier, the present work clearly demonstrates that hydrogenations of thiophene on Pt(111) do not reduce the energy barrier for the C–S bond cleavage.

KEYWORDS: desulfurization, thiophene, hydrodesulfurization on Pt(111), organosulfur compounds, C–S bond, hydrogenation



1. INTRODUCTION

Small amounts of sulfur in gasoline and diesel are increasingly demanded to meet the global environmental regulations; the deep desulfurization of sulfur-containing hydrocarbons has attracted widespread attention.^{1–3} In the petroleum industry, hydrodesulfurization (HDS) is one of the most important processes to produce clean fuels, and CoMo and NiMo sulfides are widely used as conventional HDS catalysts that can adequately desulfurize aliphatic sulfur compounds.^{3–6} However, these Mo-based catalysts are apparently less effective in treating aromatic thiophene and its derivatives, especially 4,6-dimethyl-dibenzothiophene (4,6-DMDBT), to achieve the so-called deep HDS.^{3,7,8} A great deal of research has been focused on the improvement of more effective HDS catalysts to remove S from thiophenic compounds. Recently, development of highly active HDS catalysts (e.g., supported noble metal catalysts,^{9–11} which are more active than the commercial CoMo and NiMo materials) to produce fuels with much low sulfur contents has been claimed in the petroleum industry. The key step of the desulfurization process is the C–S bond cleavage, which is still not well understood. For the rational improvement of the HDS catalysts, a detailed investigation of the desulfurization mechanism over noble metal surfaces is necessary.

The HDS mechanisms of thiophenic compounds have been discussed in a number of reviews,^{1,4,12–14} and the general conclusion is made that there exist two different reaction pathways that may compete with each other. The first one is termed the hydrogenation (HYD) pathway, initiated by hydrogenation and followed by S removal. In contrast, in the second one (termed the direct desulfurization (DDS) pathway), S is removed from thiophene without the prior hydrogenation. Owing to its relatively simple structure, thiophene is often used as a model molecule for studying the catalytic C–S bond scission and HDS mechanism. Recently, Moses et al. performed a detailed DFT investigation of thiophene on both MoS₂ and Co-promoted MoS₂.^{15,16} They pointed out that the DDS pathway is less important than the HYD pathway for MoS₂, which is in accordance with the important clues of the HYD pathway obtained from scanning tunneling microscopy studies,¹⁷ and the net effect of Co promotion was found to increase the hydrogenation activity. In contrast, because of the steric hindrance of the methyl groups, desulfurization of 4,6-DMDBT takes place mainly via the HYD

Received: May 17, 2011

Revised: August 8, 2011

Published: September 23, 2011

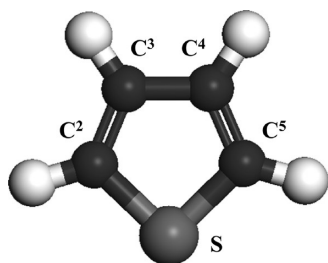


Figure 1. Schematic diagram of the thiophene molecule showing the labeling convention for the constituent atoms used in the text. The letter x in C^x represents the position of the C atom in the thiophene ring.

route,^{7,12} and the hydrogenation ability of the catalyst is of critical importance for deep HDS. Supported noble metals are much better hydrogenation catalysts than metal sulfides,^{18,19} but are easily poisoned by sulfur. The sulfur resistance can be improved by alloying¹¹ and by using an acidic support.²⁰

Platinum, the representative of noble metals, is an effective hydrogenation catalyst for many petrochemical processes.²¹ When supported on zeolites⁹ and related acidic materials (such as mesoporous silicate),¹⁰ platinum exhibits high activity toward the HDS of organic sulfur compounds, making it a potential second-generation catalyst for deep HDS. The Pt(111) surface is often considered because it is the thermodynamically most stable surface that dominates in large particles used in the catalysts. Different from the nonselective decomposition of thiophene on Mo(100),²² Mo(110),²³ Re(0001),²⁴ and Ru(0001),²⁵ yielding atomic sulfur, carbon, and H₂ as the products, ultrahigh vacuum (UHV) experiments have demonstrated that butadiene can be also formed on Pt(111)^{26,27} (also, Pd(111)²⁸ and Rh(111)²⁹), which reflects the high hydrogenation activity of platinum.

Despite these efforts, to our knowledge, no theoretical reports are available to illustrate the adsorption and HDS mechanism of thiophene on Pt surfaces. Furthermore, the effect of hydrogenation on the C–S bond cleavage of thiophene has not been clarified. These facts motivate us to perform a theoretical investigation of the desulfurization and hydrogenation processes of thiophene and its hydrogenated derivatives on Pt(111) based on the periodic, self-consistent DFT calculations. We address both the structures and energies of the involved intermediates, present detailed potential energy surfaces (PES) for the title reactions, and discuss the HDS mechanism of thiophene.

2. COMPUTATIONAL DETAILS

The DFT calculations were performed with the program package of DMol³ in the Materials Studio of Accelrys, Inc.^{30–32} The exchange–correlation energy was calculated within the generalized gradient approximation (GGA) using the form of the functional proposed by Perdew and Wang,^{33,34} usually referred to as Perdew–Wang 91. To take the relativity effect into account, the density functional semicore pseudopotential method was employed for the Pt atoms, and the carbon, sulfur, and hydrogen atoms were treated with an all-electron basis set. The valence electron functions were expanded into a set of numerical atomic orbitals by a double–numerical basis with polarization functions (DNP). A Fermi smearing of 0.136 eV and a real-space cutoff of 4.5 Å were used to improve the computational performance. All computations were performed with spin polarization.

The lattice constant of the bulk platinum was calculated to be 4.006 Å, in good agreement with the experimental value (3.912 Å).³⁵ This calculated lattice constant was subsequently used in all calculations to maintain a true energy minimum with respect to the bulk Pt reference state. The Pt(111) surface was modeled by a four-layer slab with nine platinum atoms per layer representing a $p(3 \times 3)$ unit cell, and a vacuum region of 14 Å thickness was used to separate the surface from its periodic image in the direction along the surface normal. The reciprocal space was sampled by a grid of $(3 \times 3 \times 1)$ k-points generated automatically using the Monkhorst–Pack method.³⁶ A single adsorbate was allowed to adsorb on one side of the (3×3) unit cell, corresponding to a surface coverage of 1/9 ML. Full-geometry optimization was performed for all relevant adsorbates and the uppermost two layers without symmetry restriction, while the bottom two layer Pt atoms were fixed at the positions at the calculated lattice constant. The tolerances of energy, gradient, and displacement convergence were 2.721×10^{-4} eV, 5.442×10^{-2} eV/Å, and 5×10^{-3} Å, respectively.

At the present theoretical level, the average S–Pt bond length was calculated to be 2.303 Å for S adsorbed at a fcc site, which agrees well with the low-energy electron diffraction result of 2.28 ± 0.03 Å.³⁷ The adsorption energies for S at fcc and hcp sites on Pt(111) were calculated to be 4.72 and 4.48 eV, compared with the respective values of 4.54 and 4.26 eV calculated using the GGA-PBE functional and designed nonlocal pseudopotentials implemented in the CPMD code³⁸ and 4.94 and 4.75 eV calculated using the GGA-PBE96 functional and all-electron full-potential linearized augmented plane-wave potential in the WIEN2k code.³⁹ Moreover, the calculated geometrical parameters of the gas-phase thiophene are almost the same as the experimental values (the largest difference is 0.015 Å).⁴⁰

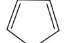
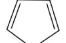
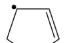
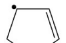








Transition state (TS) searches were performed at the same theoretical level with the complete LST/QST method.^{30–32,41} In this method, the linear synchronous transit (LST) maximization was performed, followed by an energy minimization in directions conjugating to the reaction pathway to obtain an approximated TS. The approximated TS was used to perform quadratic synchronous transit (QST) maximization, and then another conjugated gradient minimization was performed. The cycle was repeated until a stationary point was located. The convergence criterion for the TS searches was set to 0.272 eV/Å for the root-mean-square of atomic forces. Vibrational frequencies were calculated for all the initial (IS) and final (FS) states as well as the TSs from the Hessian matrix with the harmonic approximation, and zero-point energy (ZPE) was calculated from the resulting frequencies.

3. RESULTS

This part is divided into two sections. In section 3.1, we give structures and energies for the stable adsorptions of thiophene and its hydrogenated derivatives on Pt(111). In section 3.2, we investigate the desulfurization and hydrogenation steps of thiophene and its hydrogenated derivatives to gather a general view of the HDS network. For clarification, all energies reported herein are after ZPE corrections.

3.1. Adsorptions of Thiophene and Its Hydrogenated Derivatives. In this section, we present a detailed investigation of structures and energies for thiophene and its hydrogenated derivatives on Pt(111) at a surface coverage of 1/9 ML. The labeling convention for atoms in the thiophene ring, which is also

Table 1. Adsorption Sites, Adsorption Energies (ΔE_{ads} , eV), and Bond Lengths (Å) for Adsorbed Thiophene and Its Hydrogenated Derivatives on Pt(111)

species ^a	molecule	sites	ΔE_{ads}^b	$d(\text{C}-\text{Pt})$	$d(\text{S}-\text{Pt})$	$d(\text{C}^2-\text{S})$	$d(\text{C}^5-\text{S})$	$d(\text{C}^2-\text{C}^3)$	$d(\text{C}^3-\text{C}^4)$	$d(\text{C}^4-\text{C}^5)$
Thiophene _{gas}		-	-	-	-	1.729	1.729	1.374	1.422	1.374
Thiophene*		cross-bridge	1.51	2.132/2.237/2.246/2.133	2.306	1.862	1.863	1.475	1.420	1.474
		bridge-fcc	1.55	2.114/2.115	2.343	1.838	1.840	1.462	1.369	1.462
		bridge-hcp	1.55	2.115/2.115	2.345	1.840	1.840	1.462	1.368	1.463
2-MHT _{gas}		-	-	-	1.854	1.746	1.496	1.380	1.397	
2-MHT*		fcc	2.66	2.093/2.199/2.326	2.343	1.850	1.858	1.506	1.417	1.472
		hcp	2.66	2.089/2.194/2.325	2.341	1.852	1.858	1.506	1.419	1.473
3-MHT _{gas}		-	-	-	1.730	1.762	1.495	1.502	1.344	
3-MHT*		fcc	2.98	2.070/2.189/2.246	2.339	1.871	1.804	1.527	1.508	1.413
		hcp	2.99	2.072/2.189/2.246	2.343	1.871	1.804	1.526	1.509	1.413
2,3-DHT _{gas}		-	-	-	1.863	1.761	1.551	1.505	1.339	
2,3-DHT*		fcc	1.50	2.197/2.220	2.363	1.867	1.801	1.538	1.511	1.416
		hcp	1.51	2.198/2.234	2.354	1.860	1.804	1.541	1.515	1.414
2,5-DHT _{gas}		-	-	-	1.850	1.851	1.497	1.336	1.497	
2,5-DHT*		cross-bridge	1.61	2.219/2.221	2.356	1.851	1.852	1.508	1.414	1.509
		fcc	2.14	2.111/2.111	2.359	1.843	1.843	1.523	1.522	1.524
		hcp	2.12	2.119/2.119	2.363	1.842	1.843	1.524	1.521	1.524
THT _{gas}		-	-	-	1.842	1.841	1.542	1.549	1.543	
THT*		top	1.60	-	2.327	1.843	1.843	1.532	1.557	1.532

^a MHT, DHT, and THT represent monohydrothiophene, dihydrothiophene, and tetrahydrothiophene, respectively. ^b Adsorption energies are calculated using the equation: $\Delta E_{\text{ads}} = E_{\text{ads}} + E_{\text{M}} - E_{\text{ads}/\text{M}}$, where ΔE_{ads} is the adsorption energy of an adsorbate on the metal surface, $E_{\text{ads}/\text{M}}$ is the energy of the adsorbate–M adsorption system, and E_{ads} and E_{M} are the energies of the free adsorbate and the clean slab, respectively. All the energies are after zero-point energy corrections.

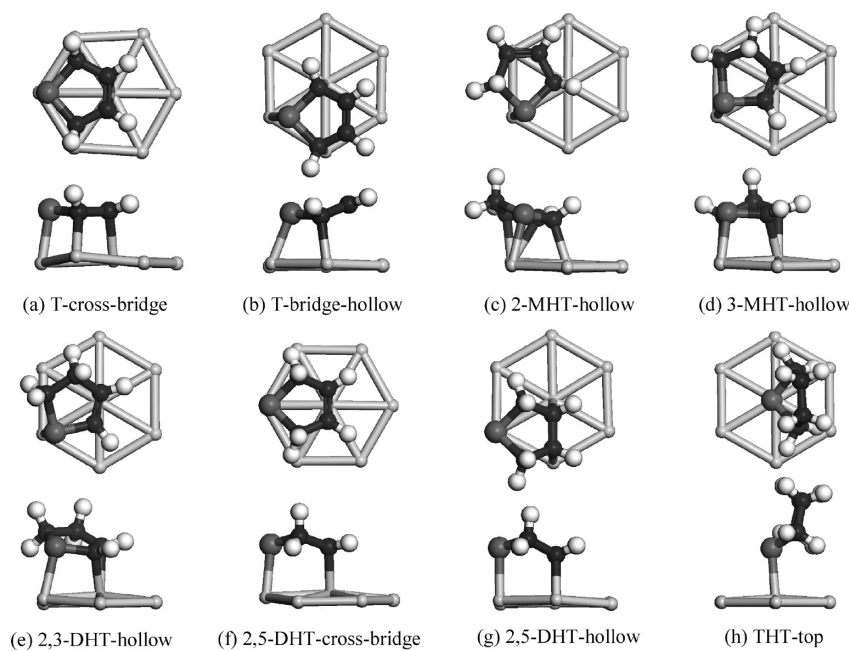


Figure 2. The most stable adsorption structures of thiophene and its hydrogenated derivatives on Pt(111). T, MHT, DHT, and THT are the abbreviations of thiophene, monohydrothiophene, dihydrothiophene, and tetrahydrothiophene, respectively. The C, S, H, and Pt atoms are shown in the black, dark-gray, white, and light-gray colors, respectively.

applied to its hydrogenated derivatives, is shown in Figure 1. The adsorption energies and some important geometric parameters of the relevant species are given in Table 1, and the representative adsorption configurations are shown in Figure 2.

3.1.1. Thiophene (T). As shown in Figure 2a,b, two types of adsorption configurations, cross-bridge and bridge-hollow (including bridge-fcc and bridge-hcp), are found for thiophene

on Pt(111). Although these configurations give almost the same adsorption energies (see Table 1), differences existing in the adsorption structures are obvious. In the cross-bridge configuration (see Figure 2a), the molecule is flat located, in agreement with the near-edge X-ray absorption fine structure, X-ray photoelectron spectroscopy (XPS), and high-resolution electron energy loss spectroscopy (HREELS) observations.^{26,27} Compared

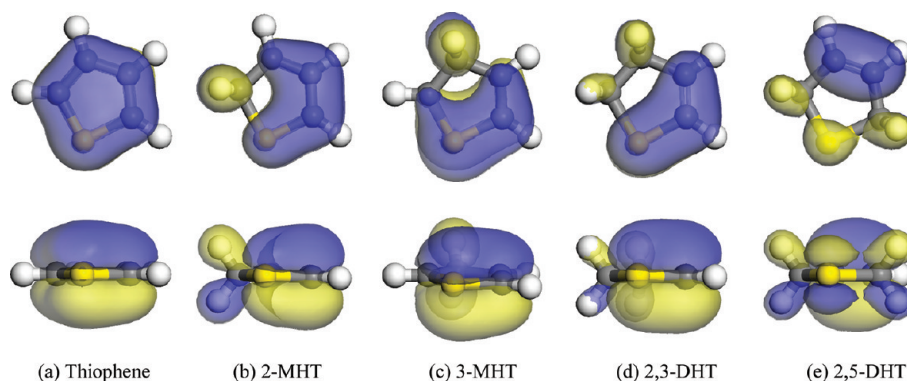


Figure 3. Schematic pictures of the π orbital of thiophene and its hydrogenated derivatives in the gas phase.

with the gas-phase values, the C^2-C^3 and C^4-C^5 bonds in the adsorption state are stretched by ~ 0.1 Å, and the $C-S$ bonds are elongated by ~ 0.13 Å, reflecting the loss of aromaticity of the molecule caused by adsorption. Furthermore, a tilted adsorption configuration of thiophene was also proposed in experiments,^{26,27} and confirmed by our calculations that the plane of the molecule is distorted in the bridge-fcc (see Figure 2b) and bridge-hcp configurations, and the $C^2C^3C^4C^5$ plane tilts from the metal surface at an angle of 22° , compared with the experimental value of $\sim 40^\circ$.²⁶ Three new bonds (C^2-Pt , C^5-Pt , and $S-Pt$) are formed (η^3 mode), in agreement with the experimental result by Lang et al.,²⁷ representing a compromise between the π interaction of the adsorbate ring with the surface (η^5 mode) and the formation of a single thiophene–platinum bond via the sulfur atom (η^1 mode). The C^2-C^3 , C^4-C^5 , C^2-S , and C^5-S bonds are elongated, as expected; however, the extents of the elongations are smaller than those in the cross-bridge configuration (see Table 1), which might be explained by the fact that in this case, the thiophene ring does not fully interact with the surface. The larger stretching of the $C-S$ bonds indicates the cross-bridge adsorption indeed weakens the $C-S$ bonds to a larger extent and thus favors the rupture of the bonds. We also note that, compared with the gas value, the C^3-C^4 bond length in the cross-bridge configuration remains almost unchanged (0.002 Å), whereas in the bridge-hollow state, it shrinks remarkably (ca. 1.37 Å) as a result of the formation of a double bond.

DFT investigations of thiophene adsorption on Ni(100),⁴² Ni(110),⁴³ Al(111),⁴⁴ Pd(100),⁴⁵ Cu(100),⁴⁵ and (Co-promoted) MoS₂^{15,16} have been published. On Ni(100), a strong chemisorption of thiophene was observed ($\Delta E_{\text{ads}} = 2.57$ eV), in which direct disruption of the aromatic ring is caused by the breaking of one of the $C-S$ bonds. However, on Ni(110), Pd(100), Al(111), and Cu(100), thiophene adsorbs molecularly in a flat manner, with the adsorption energies of 2.42, 2.20, 0.54, and 0.47 eV, respectively; the calculated adsorption structures on these surfaces are in reasonable agreement with the results obtained in the X-ray absorption fine structure and angle-resolved UV photoemission spectroscopy experiments.^{44,46–49} It is worth mentioning that thiophene could easily desorb from Cu(100), in contrast to the direct dissociation on Ni(100).⁵⁰ For (Co-promoted) MoS₂ at typical HDS conditions, thiophene adsorbs at Mo and S edges (or Co–Mo–S edge) with an adsorption energy of ~ 0.07 eV.^{15,16,51} On Pt(111), the calculated adsorption energy for thiophene is ~ 1.53 eV (see Table 1), between the values for Ni(100), Ni(110), Pd(100), Al(111), Cu(100), and (Co-promoted) MoS₂ (0.07–2.57 eV). Although the DFT results regarding the adsorption energies of thiophene on metals and

sulfides are very limited by far, we assume that the Sabatier principle, that is, the interaction between catalyst and adsorbate should be neither too strong nor too weak, works in this case, which might partially explain why the Pt metal is the proper catalyst for thiophene desulfurization.

3.1.2. Monohydrothiophene (MHT). Adding the first hydrogen atom to thiophene produces MHT, including 2- and 3-MHT, and in the gas phase, 2-MHT is 0.45 eV more stable than 3-MHT on the basis of the calculated total energies. The addition of H destroys the aromaticity of thiophene, but the remaining parts of 2-MHT (C^3 , C^4 , C^5 , and S) and 3-MHT (C^2 , C^4 , C^5 , and S) retain partial property of π -bond system, as shown in Figure 3b,c. Thus, compared with the parameters in thiophene, the C^3-C^4 , C^4-C^5 , and C^5-S bonds in 2-MHT change slightly (ca. 0.03 Å) but the other bonds stretch noticeably (ca. 0.12 Å). In 3-MHT, the C^4-C^5 , C^2-S , and C^5-S bonds also vary slightly (ca. 0.02 Å), with the rest bonds increasing by ~ 0.10 Å.

When adsorbed on Pt(111), both MHTs prefer to adsorb at a hollow site, as shown in Figure 2c,d, with adsorption energies of 2.66 (2-MHT) and 2.98 (3-MHT) eV; the molecule plane is essentially flat except for the slight uplift of the CH₂ group, and the S atom sits at the top site. Moreover, compared with the relevant gas values, the C^3-C^4 , C^4-C^5 , and C^5-S bonds in 2-MHT increase by ~ 0.08 Å while the other bond lengths undergo relatively small changes (ca. 0.01 Å). For 3-MHT, the C^4-C^5 , C^2-S , and C^5-S bonds increase by ~ 0.08 Å while the variation in the other bonds is small (ca. 0.02 Å). These facts indicate that the adsorptions further weaken the π -bond system of MHTs.

3.1.3. Dihydrothiophene (DHT). In the previous studies, only 2,3- and 2,5-DHT were taken as the intermediates involved in the HDS process.^{1,15,16,52,53} Thus, for simplicity, we consider only these two DHT's. DHT is formed after the addition of a hydrogen atom to MHT, and the π -bond system is further depleted, including only the C^5-S and C^4-C^5 bonds in 2,3-DHT and the C^3-C^4 bond in 2,5-DHT, which can be seen from the shrinking of the π orbital (see Figure 3d,e). In the gas phase, compared with the relevant parameters of thiophene, the average variation of the C^5-S and C^4-C^5 bonds in 2,3-DHT is small (ca. 0.03 Å) but the other bonds increase by ~ 0.13 Å; in 2,5-DHT, the C^3-C^4 bond is shortened by 0.09 Å for the formation of the double bond while the rest bonds are stretched by more than 0.12 Å.

As shown in Figure 2e, the most stable adsorption of 2,3-DHT is at fcc and hcp sites, gaining energies of ~ 1.50 eV. The molecule plane is tilted, which is caused by the uplift of the two adjacent CH₂ groups, and the S atom of 2,3-DHT stays at top site; however,

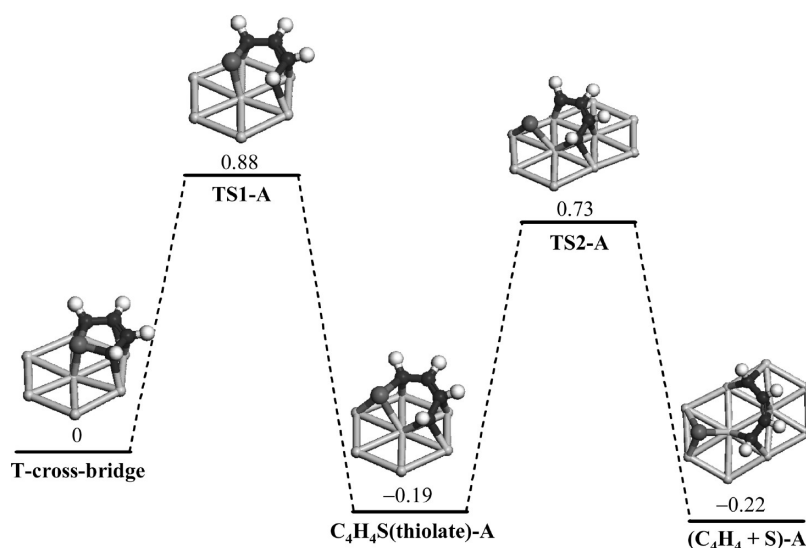


Figure 4. Desulfurization pathway of thiophene from the T-cross-bridge adsorption configuration on Pt(111). TS represents the transition state. The energy reference corresponds to the total energy of T-cross-bridge plus four atomic H adsorbed at infinitely separated sites on the slab. The atomic H's adsorbed at infinitely separated sites on the slab are omitted for simplicity.

2,5-DHT forms two types of adsorption modes on Pt(111), which are at cross-bridge and hollow (fcc and hcp) sites. The S atom of 2,5-DHT also sits at the top site. Except for the adsorption site, as shown in Figure 2f,g, the difference between these adsorption configurations is small. The adsorption energies at the cross-bridge, fcc, and hcp sites are 1.61, 2.14, and 2.12 eV, respectively. Compared with the gas-phase parameters, adsorption of 2,3-DHT on Pt(111) leads to relatively large stretches in the C⁵–S and C⁴–C⁵ bonds (ca. 0.06 Å) and small changes in the C²–S, C²–C³, and C³–C⁴ distances (ca. 0.01 Å), indicating the π -bond system of 2,3-DHT is further destroyed. For 2,5-DHT, the adsorption results in an obvious increase in the C³–C⁴ bond length (ca. 0.15 Å) and small change in the other bonds (ca. 0.02 Å), reflecting the π bond between C³ and C⁴ is, indeed, weakened in the adsorption state.

3.1.4. Tetrahydrothiophene (THT). The addition of four H atoms to thiophene completely destroys the π -bond system. Compared with the relevant parameters of thiophene, all the C–S and C–C bonds in THT are elongated by more than 0.1 Å. As shown in Figure 2h, THT prefers the top site through the S atom with the adsorption energy of 1.60 eV. The adsorbed THT has actually taken off from the metal surface, and the S atom is out of the C²C³C⁴C⁵ plane. The adsorption of THT leads to small changes in all the C–S and C–C bond lengths (less than ca. 0.01 Å). The especially small change in the C–S bond lengths (by only ca. 0.002 Å) indicates that the adsorption process may have little effect on the C–S bond scission of THT.

3.2. Reaction of Thiophene and Its Hydrogenated Derivates. Stöhr et al.²⁶ and Lang et al.²⁷ have shown in their X-ray and HREELS studies that the C–S bond cleavage in thiophene begins at around 290 K, and the removal of the S atom from the ring starts at 350 K; the final products include H₂, C, S, and butadiene. In this section, we present the desulfurization pathways of thiophene and its hydrogenated derivatives, together with the hydrogenation pathways of thiophene into 2,3- and 2,5-DHT, and the formation of butadiene. Since similar adsorption structures and energies are obtained at bridge-fcc and bridge-hcp sites for thiophene and at fcc and hcp sites for the hydrogenated derivatives of thiophene, we choose the adsorptions of thiophene

at the bridge-fcc site and 2-MHT, 3-MHT, 2,3-DHT, and 2,5-DHT at the fcc site to represent the corresponding bridge-hollow and hollow adsorption configurations in the investigation of the desulfurization of the intermediates. The details regarding the change in the C–S distances during the desulfurization process are given in Table S1 of the Supporting Information.

3.2.1. Desulfurization of Thiophene. The calculated results of Section 3.1 have shown that the C–S bond cleavage in thiophene might occur more readily from the cross-bridge configuration because in that case, the relevant bond is weakened to a larger extent. Thus, we determine the desulfurization processes of thiophene from that state. The calculated desulfurization PES of cross-bridge adsorbed thiophene is displayed in Figure 4 with the corresponding schematic structures involved, and the initial configuration is taken as the energetic reference.

The desulfurization process for the cross-bridge configuration of thiophene involves two sequent C–S bond scissions. The first C–S (C⁵–S) bond cleavage involves movement of the S atom toward the adjacent bridge site forming bond with another surface Pt atom. In the TS of this step (TS1-A), the C⁵–S bond is ruptured. After TS1-A, a stable intermediate, C₄H₄S(thiolate), is formed as the FS in which both the C⁵ and S atoms stay at bridge sites with the C⁵–S distance further elongated. The adsorption structure of C₄H₄S when the Pt atom is included in the 6-member ring is similar to that found in the organometallic reaction, in which the metal atom inserts into the C–S bond of thiophene.^{1,54} This step accounts for an activation barrier of 0.88 eV and a reaction energy of -0.19 eV. The second C–S bond cleavage is activated with the help of the C–S bond-stretching vibration, producing coadsorbed C₄H₄ and S. In the TS of this step (TS2-A), the S and C² atoms still sit at the bridge and top sites, respectively, but the C²–S bond is ruptured. After TS2-A, the C² atom moves to the bridge site, and the S atom shifts to its most stable (hollow) site,⁵⁵ forming the FS ((C₄H₄ + S)-A). The activation barrier of this step is 0.92 eV, and the reaction energy is -0.03 eV. A similar desulfurization process of bridge-fcc adsorbed thiophene is also determined, and the corresponding PES is given in Figure S1 of the Supporting Information.

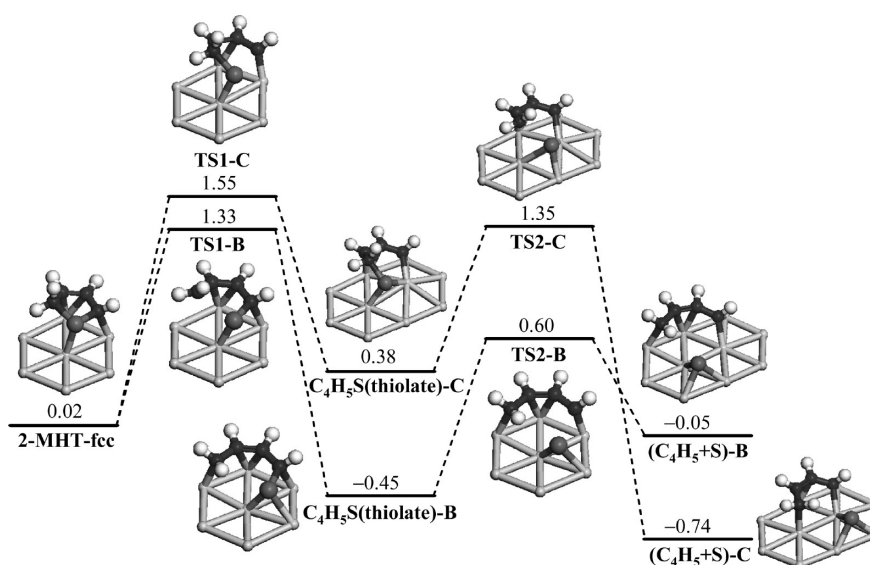


Figure 5. Desulfurization pathway of 2-monohydrothiophene at the fcc site on Pt(111) (2-MHT-fcc). Parameters follow the same notation as in Figure 4.

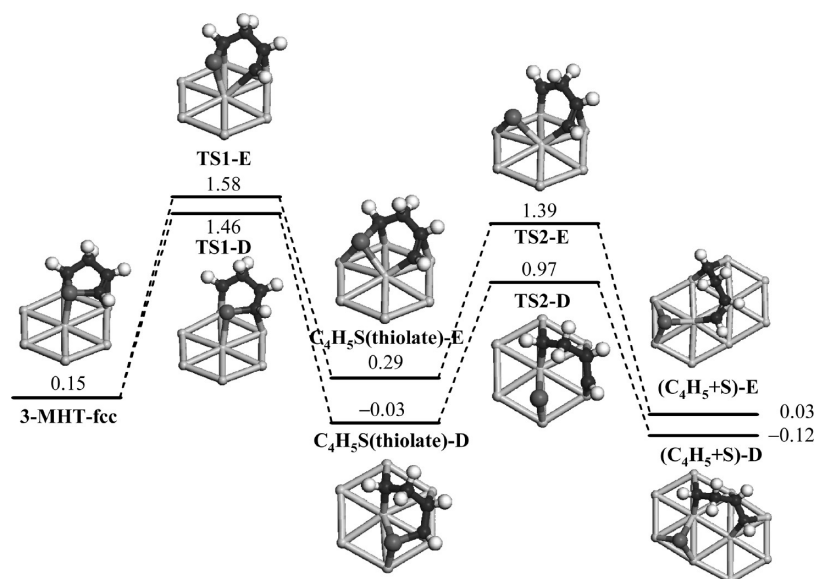


Figure 6. Desulfurization pathway of 3-monohydrothiophene at the fcc site on Pt(111) (3-MHT-fcc). Parameters follow the same notation as in Figure 4.

3.2.2. Desulfurization of MHT. In this part, we explore the desulfurization of MHT's (2- and 3-MHT). The corresponding PES's together with the schematic structures involved are presented in Figures 5 and 6.

2-MHT, as shown in Figure 2c, has two different C–S bonds and, thus, has two desulfurization paths, according to the C–S bond scission sequence. Here, we define the path, which begins with the C²–S bond scission, as path B; and the other path, starting with the breaking of the C⁵–S bond, as path C. Path B is more favorable than path C because of the lower C–S bond cleavage barrier involved. In path B, as shown in Figure 5, intrarotation of the CH₂ group along the C²–C³ axis facilitates interaction between C² and the surface so that the C²–S bond is activated. The energy barrier of this step is 1.31 eV, and the reaction energy is –0.47 eV. The second

step is the C⁵–S bond cleavage, which results from the stretching vibration of the involved bond. This step accounts for an activation barrier of 1.05 eV and a reaction energy of 0.4 eV.

3-MHT also has two kinds of reaction paths according to the C–S bond scission sequence. We define the path beginning with the C²–S bond scission as path D; and the path starting with the rupture of the C⁵–S bond as path E, as shown in Figure 6. Path D is more favorable than path E because of the lower C–S bond cleavage barrier involved. For path D, the initial C²–S bond scission is facilitated by a swag vibration of the C²H group, leading to the movement of the C² atom toward the adjacent bridge site. The energy barrier of this step is 1.31 eV, and the reaction energy is –0.18 eV. In the second step, the C⁵–S bond scission is due to the C⁵–S stretching vibration. This step

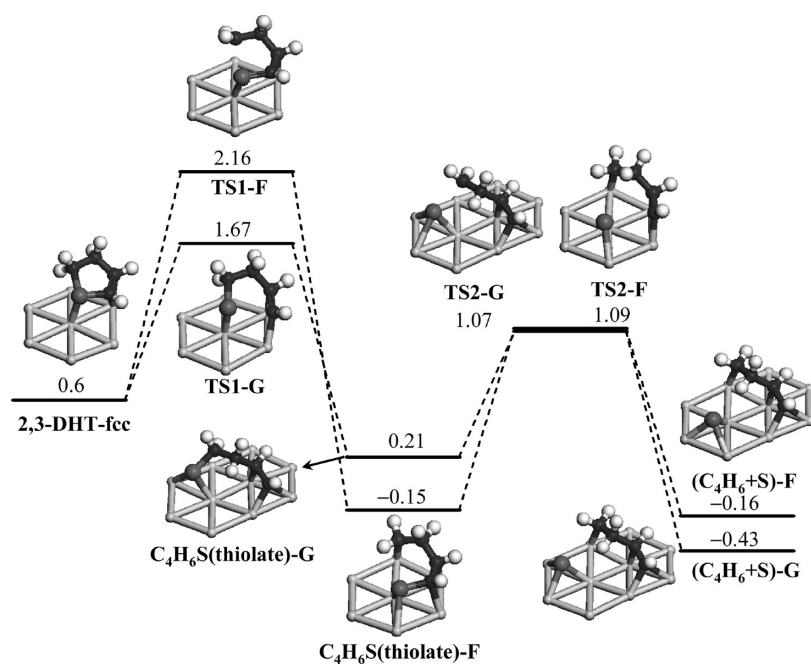


Figure 7. Desulfurization pathway of 2,3-dihydrothiophene at the fcc site on Pt(111) (2,3-DHT-fcc). Parameters follow the same notation as in Figure 4.

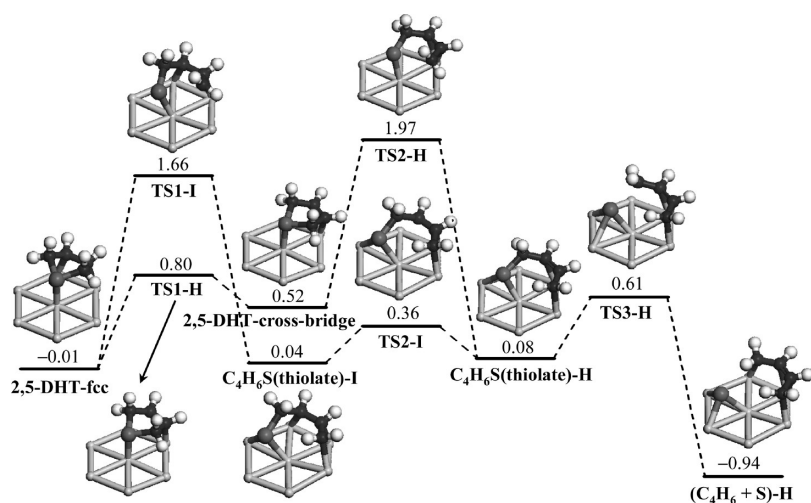


Figure 8. Desulfurization pathway of 2,5-dihydrothiophene at the fcc site on Pt(111) (2,5-DHT-fcc). Parameters follow the same notation as in Figure 4.

accounts for an activation barrier of 1.00 eV and a reaction energy of -0.09 eV.

In summary, two competitive paths are involved in the desulfurization of MHT's, and the path with the initial rupture of the C–S bond close to the CH₂ group is more favorable. This might be explained by the steric effects. For 2-MHT, because the C² atom is not involved in a surface bond, the deformation of 2-MHT caused by the C²–S bond scission proceeds more easily than by the C⁵–S bond scission; moreover, the FS of the C⁵–S bond scission (C₄H₅S(thiolate)-C) is less stable than that of the C²–S bond scission (C₄H₅S(thiolate)-B) because obvious surface corrugation is involved in C₄H₅S(thiolate)-C, in which the Pt atom lifts up from the metal surface because it is bound to both the C⁵ and S atoms. For 3-MHT, the process of the initial C²–S

bond scission is accompanied by a change in the hybridization of the C⁴ and C⁵ atoms from sp² to sp³, leading to strong interaction with the metal surface, whereas the hybridization situation does not alter in the initial C⁵–S path. In addition, the initial C⁵–S bond scission also causes significant surface corrugation, making C₄H₅S(thiolate)-E unstable. Thus, the initial C²–S bond scission is favored for 3-MHT, as well.

3.2.3. Desulfurization of DHT. This part is dedicated to the investigation of the desulfurization mechanism of DHT's (2,3- and 2,5-DHT). The corresponding PES's together with the schematic structures involved are shown in Figures 7 and 8, respectively.

2,3-DHT, as shown in Figure 2e, gives two different C–S bonds (H₂C–S and HC–S) and, thus, has two kinds of desulfurization

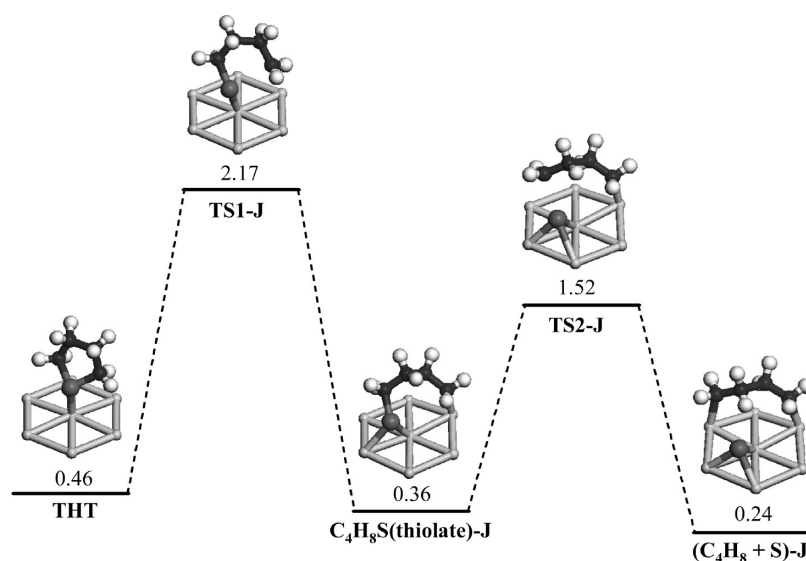


Figure 9. Desulfurization pathway of tetrahydrothiophene (THT) on Pt(111). Parameters follow the same notation as in Figure 4.

paths, according to the different C–S bond scission sequences. Here, we define the path that begins with the H₂C–S (C²–S) bond scission as path F and the path starting with the rupture of the HC–S (C⁵–S) bond as path G (see Figure 7). Compared with path F, path G is more favorable, based on the relevant energy barriers and total reaction energies. In path G, the C⁵–S bond scission results from a swag vibration of the C⁵H group. The energy barrier of this step is 1.07 eV, and the reaction energy is –0.39 eV. The second step is facilitated by the intrarotation of the C²H₂ group along the C²–C³ axis. The barrier of this step is 0.86 eV, and the reaction energy is –0.64 eV. Note that, in contrast to the situation of MHT, 2,3-DHT prefers to first break the C⁵–S bond, which is far away from the CH₂ groups.

2,5-DHT, as shown in Figure 2f,g, has two types of adsorption configurations (cross-bridge and hollow). Similar to the situation of thiophene desulfurization (Section 3.2.1), the fcc and hcp configurations have similar adsorption properties (see Table 1); thus, for simplicity, we use the fcc configuration to represent the hollow adsorption structure. The desulfurization process of 2,5-DHT on Pt(111), which involves two paths, is shown in Figure 8. Path H starts with the conversion of 2,5-DHT from the fcc site to the cross-bridge site, followed by the C⁵–S and C²–S bond scission, and path I includes the C⁵–S bond scission in the fcc adsorbed 2,5-DHT and a surface isomerization process that incorporates path I into path H at C₄H₆S(thiolate)-H. Compared with path I, path H is more favorable because of the relatively low energy barrier involved. In path H, the energy barrier for the fcc-to-cross-bridge conversion of 2,5-DHT is 0.81 eV. The second step is the cleavage of the C⁵–S bond, motivated by the intrarotation of the C⁵H₂ group along the C⁴–C⁵ axis. The activation barrier of this step is 1.45 eV, and the reaction energy is –0.44 eV. The final step is the C²–S bond cleavage, which is also motivated by the intrarotation of the relevant CH₂ group. This step accounts for an energy barrier of 0.53 eV and a reaction energy of –1.02 eV.

3.2.4. Desulfurization of THT. The desulfurization PES of THT together with the schematic structures involved is shown in Figure 9. The barrier of the first C⁵–S bond scission step is 1.71 eV, and the reaction energy is –0.1 eV. The second step is the

C²–S bond scission, producing coadsorbed C₄H₈ and S. This step accounts for an energy barrier of 1.07 eV and a reaction energy of –0.12 eV. It should be pointed out that both the C–S bond scissions are activated with the help of the intrarotation of the corresponding CH₂ group.

3.2.5. Hydrogenation of Thiophene. Hydrogenation and C–S bond cleavage may compete with each other in the HDS processes of thiophene. In the above sections (3.2.1–3.2.4), we mainly illustrated the desulfurization processes of thiophene, MHT, DHT, and THT on Pt(111). To explore the HDS mechanism of thiophene, we need to further study thiophene hydrogenations. Considering the complexity of reactions caused by various possible hydrogenation positions in thiophene and its hydrogenated derivatives and for simplicity, we calculate only the hydrogenation processes from thiophene to 2,3-DHT and 2,5-DHT via 2-MHT and 3-MHT. PES together with the schematic structures involved in the hydrogenation of thiophene (bridge-fcc) to 2,3-DHT (fcc) and 2,5-DHT (cross-bridge and fcc) is shown in Figure 10. Here, we define the paths starting with the addition of H to positions 2 and 3 of thiophene as paths K and L, respectively. The hydrogenation PES of thiophene (cross-bridge) to 2-MHT and 3-MHT, together with the schematic structures involved, is presented in Figure S2 of the Supporting Information.

For path K, the first hydrogenation step yields 2-MHT. The energy barrier of this step is 1.17 eV. The second hydrogenation step involves three possibilities: the first is the addition of H to position 3 of 2-MHT, forming 2,3-DHT, with an energy barrier of 0.76 eV. The second is the H addition to position 5 of 2-MHT, forming 2,5-DHT-fcc with an energy barrier of 1.28 eV; and the last is also the H addition to position 5 of 2-MHT; however, it forms 2,5-DHT-cross-bridge, with an energy barrier of 1.47 eV. For path L, the first hydrogenation step produces 3-MHT, with an energy barrier of 0.74 eV. The second hydrogenation step involves H addition to position 2, forming 2,3-DHT, with an energy barrier of 1.44 eV.

3.2.6. Formation of Butadiene. For the final hydrogenation of C₄H₄ and S, the C–S bond scission product of T-cross-bridge ((C₄H₄ + S)-A) is chosen as the IS, which is coadsorbed on the Pt(111) surface; the hydrogenation PES is presented in Figure 11. For the S atom, the first hydrogenation step (S + H → SH, path M)

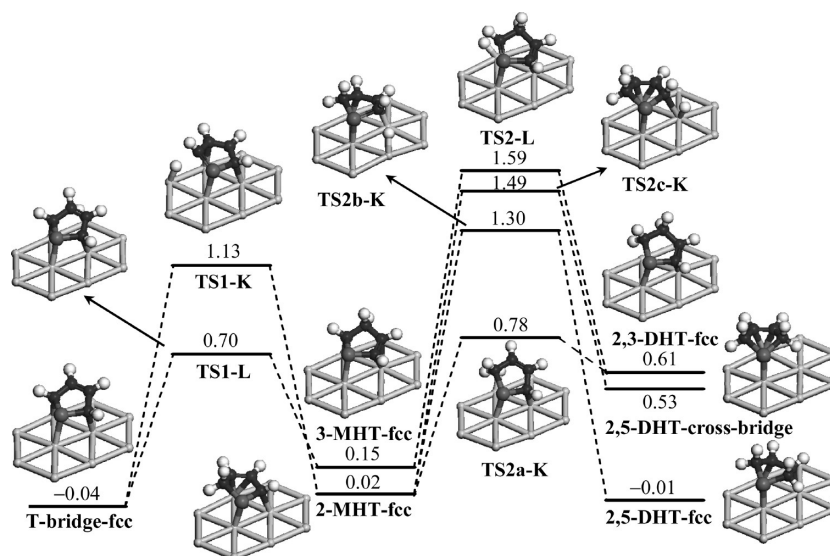


Figure 10. Hydrogenation pathways of thiophene from the bridge-fcc site on Pt(111) (T-bridge-fcc). Parameters follow the same notation as in Figure 4.

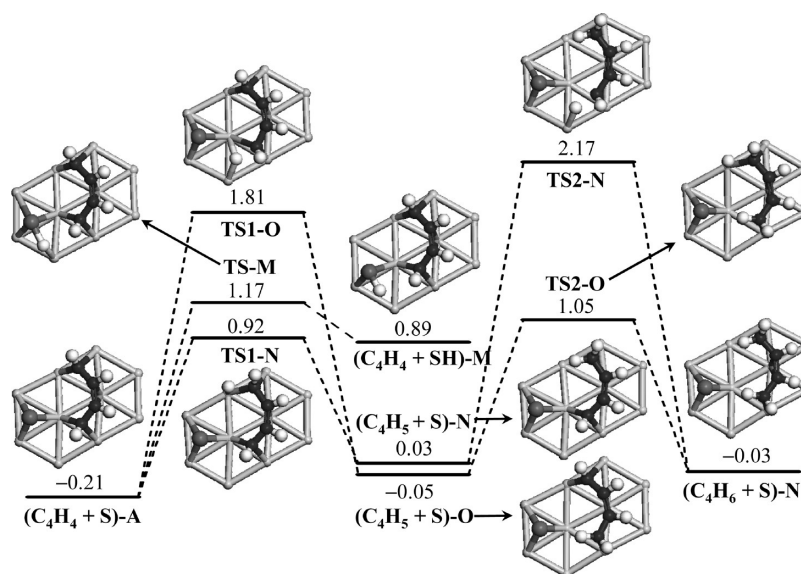


Figure 11. Hydrogenation pathways of the C-S bond scission product of T-cross-bridge (($C_4H_4 + S$)-A). Parameters follow the same notation as in Figure 4.

has an energy barrier of 1.38 eV; however, further hydrogenation of the SH group ($SH + H \rightarrow H_2S$) is unfavorable because the optimization of adsorbed H_2S definitely leads back to the isolated state ($SH^* + H^*$), indicating adsorbed H_2S is, indeed, unstable, in accordance with the DFT results on the clean Pt(111) by Michaelides and Hu.⁵⁶ For the C_4H_4 species, the hydrogenation process for the formation of *cis*-butadiene contains two paths: one starts with hydrogenation on the C^2 atom (path N), and the other begins with hydrogenation on the C^5 atom (path O). Both paths end up with the same FS (($C_4H_6 + S$)-N), and relatively high hydrogenation barriers (TS1-O, 2.02 eV; TS2-N, 2.14 eV) are involved, which may be caused by the blocking of strong adsorbed S on hydrogenation on the C^5 atom. Despite these high barriers involved, the formation of adsorbed butadiene is more favorable than that of adsorbed H_2S . Moreover, the adsorption energy of *cis*-butadiene is calculated to be

1.03 eV on the clean Pt(111) and 0.73 eV on the S-co-adsorbed Pt(111) (($C_4H_6 + S$)-N), meaning that coadsorbed S could facilitate the desorption of *cis*-butadiene from Pt(111). These results explain the UHV experimental observations^{26,27} that butadiene rather than H_2S could be formed and desorbed from Pt(111).

4. DISCUSSION

In this section, we discuss some important points based on the calculated results.

4.1. General Structural Features for Adsorbed Thiophene and Its Hydrogenated Derivatives. It is commonly accepted that the adsorption configuration of a molecule has an important influence on its reaction mechanism. After getting the stable adsorption structures of thiophene and its hydrogenated derivatives,

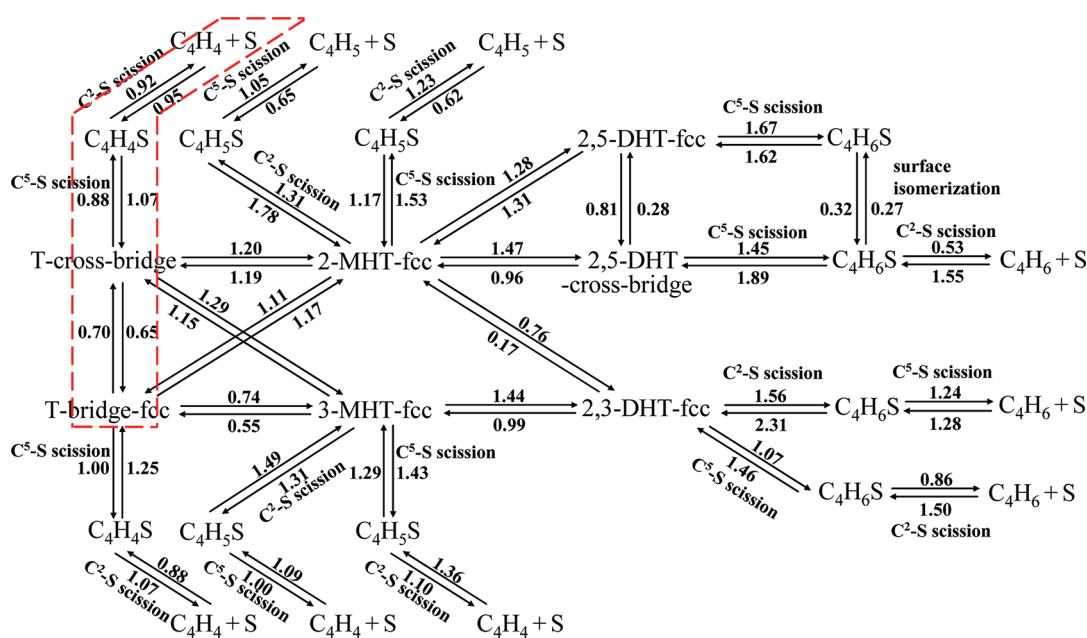


Figure 12. Desulfurization network of thiophene (T) and its hydrogenated derivatives (monohydrothiophene (MHT) and dihydrothiophene (DHT)) on Pt(111). The activation barriers (eV) of each step and its reverse process are given. For T and 2,5-DHT, the C⁵–S scission followed by C²–S scission is taken as the order of the C–S bond cleavage. For simplicity, the reactions for 2-MHT, 3-MHT, 2,3-DHT, and 2,5-DHT on the hcp sites and for thiophene on the bridge-hcp site are not given. The pathway contained in the dashed line is the most favorable desulfurization pathway for thiophene on Pt(111) (DDS pathway).

we can give a general description of hybridizations for both C and S atoms, which to a large extent determines the bonding modes within the molecule and between the molecule and the metal surface. The S atom in all the adsorbed thiophenic compounds is always sp³-hybridized because when adsorption occurs, the π -bond system of the gas-phase thiophene, 2-MHT, 3-MHT, and 2,3-DHT is destroyed and a σ bond between sulfur and a surface Pt atom would be formed, leading to the conversion of sulfur from sp² to sp³, whereas in 2,5-DHT and THT, the S atom retains its sp³ hybridization, as in the gas phase. The C atom exists in two groups: CH and CH₂. In the methylene group, the C atom is always sp³-hybridized. In the methyne group, the C atom is either sp²- or sp³-hybridized, depending on how the group interacts with the surface Pt atoms. When forming a σ bond to a surface Pt atom, the C atom is sp³-hybridized; but it would be sp²-hybridized when it interacts with the surface via the π (C=C) orbital or it does not interact with the surface, for example, the C³ and C⁴ atoms in the bridge-fcc configuration of thiophene. The hybridization of the C atom in the CH group dictates the tilting angle of the C–H axis with respect to the surface plane in the adsorbed thiophenic compounds, that is, the sp³ hybridization of C leads to a larger tilting than the sp² hybridization. A similar situation is also observed in thiophene on Ni(100),^{42,45} Ni(110),⁴³ Cu(100),⁴⁵ Pd(100),⁴⁵ and benzene on Pt(111).^{57,58}

The investigation of the change of the C–S bond lengths between thiophene and its hydrogenated derivatives in both the gas phase and adsorption state is instructive for the study of HDS mechanism. On the basis of the analysis of the bond lengths in thiophene and its hydrogenated derivatives, it is suggested that in the gas phase, the delocalized π -bond system always tries to keep the unhydrogenated parts of a molecule unchanged from the influence of hydrogenation, that is, the variation of the C–C or C–S bond length upon hydrogenation is small if the bond is included in the π -bond system; otherwise, it increases noticeably. The shrinking of the π -bond system from thiophene to its

hydrogenated derivatives shown in Figure 3 illustrates the gradual decrease in the effect of the π bond on the molecular structure during the hydrogenation process.

When adsorbed on Pt(111), the π -bond system of the molecule is destroyed because of the interaction between the d orbitals of surface Pt atoms and the π orbitals of the adsorbed molecule. It is worth noticing that, different from the stepwise damage of the π -bond system caused by hydrogenation in the gas phase, the adsorption of thiophene on Pt(111) completely destroys the π -bond system or leaves only one π bond in the molecule; that is, under the HDS conditions, the adsorption process of thiophene has already destroyed the delocalized π -bond system before hydrogenation occurs. After comparing the structural parameters in the adsorption state, we find that on going from thiophene to its hydrogenated derivatives, the C–S bond length changes slightly ($< \sim 0.02$ Å). This indicates that hydrogenation toward thiophene on Pt(111) does not have much influence on the C–S bond and, thus, may not lower the C–S bond scission barrier.

Adsorption of thiophene over Co/MoS₂ is more complicated because two different edges are involved. To probe the fundamental descriptors that determine the adsorption energy of sulfur-containing molecules, such as thiols, thiophene, and its derivatives, Joshi et al. limited the number of interactions between the adsorbate and the adsorbent and focused on the η^1 adsorption mode of both edges, in which only the S atom of the molecule interacts with the surface atoms.⁵⁹ They found that the sulfur lone pair descriptors can be used to describe the adsorption energy variation for a set of molecules and the occupancy of the lone pair orbitals for electrons on sulfur plays an important role in determining the adsorption energy. On Pt(111), however, thiophene and its hydrogenated derivatives are mainly in flat or nearly flat modes (η^3 , η^4 , and η^5 ; η^1 for only THT; see Figure 2), which means, in addition to the S atom, the

Table 2. Comparison between the Calculated Energy Barriers E_a (eV) of the C–S Bond Scission for Adsorbed Thiophene and Its Hydrogenated Derivatives on Pt(111)^a

		thiophene		2-MHT	3-MHT	2,3-DHT	2,5-DHT		THT
site		cross-bridge	bridge-fcc	fcc	fcc	fcc	cross-bridge	fcc	top
E_a	1st C–S scission	0.88	1.00	1.31	1.31	1.07	1.45	1.67	1.71
	2nd C–S scission	0.92	1.07	1.05	1.00	0.86	0.53	0.53	1.16

^a For 2-MHT-fcc, 3-MHT-fcc, and 2,3-DHT-fcc, the energy barriers of the first and second C–S bond scission are chosen from the corresponding most favorable C–S bond cleavage pathway.

C atoms generally participate in the interaction with the metal surface. Thus, the descriptors that determine the adsorption energies for thiophene and its hydrogenated derivatives on Pt(111) might not be simply attributed to the electronic structure of the S atom.

4.2. Reaction Pathways. On the basis of the calculated results, we can give the reaction network of the desulfurization of thiophene on Pt(111), as shown in Figure 12. The conversion barriers between the cross-bridge and bridge-fcc configurations of thiophene are 0.65 and 0.70 eV, respectively (the conversion PES together with the involved schematic structures is shown in Figure S3 of the Supporting Information). The DDS pathway of thiophene includes the two-step C–S bond scission with barriers of 0.88 and 0.92 eV for the T-cross-bridge configuration and 1.00 and 1.07 eV for the T-bridge-fcc configuration. Thus, under the UHV condition, the desulfurization of thiophene proceeds more readily from the T-cross-bridge configuration, in line with the C–S bond lengths (see Table 1).

When the hydrogenation conditions are considered, there are four different initial hydrogenation steps for thiophene, that is, T-cross-bridge/T-bridge-fcc hydrogenations to 2- and 3-MHT. Among them, the T-bridge-fcc to 3-MHT hydrogenation has the lowest energy barrier (0.74 eV) and, thus, appears to be the most favorable hydrogenation path. However, further reactions of 3-MHT are hindered by rather high barriers (e.g., 1.44 eV for hydrogenation to 2,3-DHT and 1.37 eV for the C–S bond scission), whereas the dehydrogenation barrier for 3-MHT back to T-bridge-fcc is only 0.55 eV. Thus, we propose that 3-MHT would prefer dehydrogenation rather than hydrogenation or C–S bond cleavage. As a result, the hydrogenation of T-bridge-fcc to 3-MHT is blocked, although the involved barrier is relatively low.

For the T-bridge-fcc configuration, conversion to the T-cross-bridge configuration is a favorable path because it involves a lower barrier (0.70 eV) with respect to the alternative C–S bond scission (1.00 eV) and hydrogenation to 2-MHT (1.17 eV). Similarly, for the T-cross-bridge configuration, the conversion to the T-bridge-fcc configuration is also preferred when the corresponding desulfurization and hydrogenation barriers are considered. Notice that on Pt(111), the T-bridge-fcc configuration is slightly more stable than the T-cross-bridge configuration, and thus, at low temperatures, thiophene prefers the bridge-fcc adsorption. With the temperature increased, thiophene would first convert into the T-cross-bridge configuration, and the C–S bond cleavage occurs subsequently. We further examine the hydrogenation of the C_4H_4S (thiolate)-A intermediate, which is the product of the initial C–S bond scission of the cross-bridge adsorbed thiophene (see Figure S4 in Supporting Information). The barrier of this step is ~ 1.47 eV, much higher than the barrier for its C–S bond scission (0.92 eV), indicating the stepwise C–S bond cleavage pathway is favored. Therefore, thiophene desulfurization on Pt(111) should proceed along the DDS pathway.

Our calculated result of the DDS pathway is in good agreement with the previous XPS and HREELS studies of thiophene on Pt(111).^{26,27} The thiophene molecule at 150 K is oriented in a tilted manner, and as the temperature increases, thiophene changes from the tilted configuration to a parallel-bonded geometry at 180 K.²⁶ This is in accordance with conversion of adsorbed thiophene from the tilted T-bridge-fcc configuration to the parallel T-cross-bridge configuration with a barrier of 0.70 eV. The C–S bond cleavage begins at around 290 K, and the removal of S starts at 350 K,^{26,27} which is in line with the calculated barriers of 0.88 and 0.92 eV for the stepwise C–S bond cleavages. Since these experiments were performed under the UHV condition, the observed desorption of H_2 and butadiene indicates that there is a small amount of adsorbed H , which comes from the dehydrogenation of the adsorbed C_4H_4 species.²⁶ However, no hydrogenated thiophenic compounds were isolated in these studies,^{1,26,27} which might be interpreted as the disfavor of the HYD pathway.

The formation of butadiene can be explained as the result of the hydrogenation toward the remaining C_4H_4 species, which has not been dehydrogenated yet. Recent DFT study of thiophene desulfurization on Ni(100) also confirms the DDS pathway by investigating the influence of hydrogenation (two H atoms addition to positions 2 and 5 of thiophene) after the initial C–S bond cleavage.⁶⁰ The hydrogenation is predicted to lower the desulfurization barrier to 0.14 eV, compared with the barrier of 0.71 eV for the DDS pathway. However, the hydrogenation barrier itself, 0.98 eV, disfavors the HYD pathway.

Since saturated organosulfur compounds are industrially more easily desulfurized than aromatics, it is generally believed that the C–S bond of aromatic organosulfur compounds would be more friable if they are hydrogenated because of the loss of aromaticity. The hydrogenation, as mentioned above, is predicted to lower the C–S cleavage barrier on Ni(100).⁶⁰ This point is also confirmed by the XPS experiments conducted by Lang et al. that the C–S bond cleavage of thiophene on Pt(100) starts at 230 K, whereas for THT, it begins at 175 K.²⁷ However, the present calculations clearly show that this is not the case for Pt(111). As shown in Table 2, with the proceeding of hydrogenations (from thiophene to THT), the first C–S bond scission barrier would increase rather than decrease (except for 2,3-DHT); the second C–S bond scission barrier changes slightly (remains around 1.00 eV, except for 2,5-DHT), indicating that hydrogenation toward thiophene on Pt(111) does not make the desulfurization process easier, in agreement with the effect of hydrogenations on the C–S bond strengths in the thiophenic compounds on Pt(111), as discussed in Section 4.1.

The LUMO of the gas-phase thiophene is the C–S antibonding orbital ($3b_1$).^{61,62} When adsorption occurs, electrons would transfer from the metal into this antibonding orbital and strongly weakens the C–S bond. For the hydrogenated derivatives,

however, the LUMO is no longer the C–S antibonding orbital and, thus, is not effectively occupied in the adsorption configurations. From this perspective, it is not surprising that hydrogenation of thiophene on Pt(111) does not help to reduce the energy barrier for the C–S bond cleavage. Note that the C–S bond cleavage of thiophene on Pt(111) begins at around 290 K;²⁶ thus, the experimental results on Pt(100) of Lang et al. might be explained by the higher activity of Pt(100) than Pt(111) toward thiophene and its hydrogenated derivatives. A detailed study on the structural sensitivity of Pt surfaces in the HDS process is underway and will be presented in our next paper.

It is interesting to compare our results on Pt(111) with the previous DFT studies for thiophene on Mo-based sulfides. On MoS₂, the HYD pathway is preferred, but on Co-promoted MoS₂, the HYD pathway is still favored, but with more importance in the DDS pathway caused by the Co promotion effect; 2,5-DHT is the most important intermediate on both MoS₂ and Co-promoted MoS₂ during the HDS process.^{15,16,53} On Pt(111), the DDS pathway becomes dominant, and the hydrogenated derivatives of thiophene, such as 2,5-DHT, could not be formed easily. Notice that the HYD pathway on Co/MoS₂, according to the DFT results of Moses et al.,^{15,16} involves multiple diffusions of intermediates between Mo- and S-edges (or Co–Mo–S edge) in addition to hydrogenation, whereas the DDS pathway on Pt(111) contains only two direct C–S scission steps, indicating the higher desulfurization efficiency of Pt compared with Mo-based sulfides. In addition, the final hydrocarbon product of thiophene HYD route on Co/MoS₂ is *cis*-2-butene, but on Pt(111), *cis*-butadiene is produced via the thiophene DDS route and the final hydrogenation steps. This fact suggests that Pt would consume less hydrogen than Co/MoS₂ in the thiophene HDS process.

In our previous DFT study of methanethiol on Pt(111),⁵⁵ we found that adsorbed CH₃SH prefers spontaneous dissociation into thiolmethoxy (CH₃S), followed by direct C–S bond scission of CH₃S under the hydrogenation condition; in this work, we find that the thiophene reaction proceeds along the DDS pathway on Pt(111), followed by hydrogenation to form butadiene with less hydrogen compared with the situation of Co/MoS₂. These results suggest that the platinum catalyst exhibits high desulfurization efficiency with low hydrogen consumption for the simple S-containing compounds. For the more complicated S-containing molecules, such as 4,6-DMDBT, the hydrogenating ability of platinum might become crucial for S removal. The methyl groups in 4,6-DMDBT, adjacent to the sulfur atom, prevent the sulfur atom from σ -binding with the catalytic site,^{7,12,63} and it is suggested that hydrogenation might result in the removal of the molecular planarity in the adsorption structure so that the S atom could reach the catalyst surface without being blocked by alkyl groups. Our calculated result of the adsorption structure of THT on Pt(111) (see Figure 2h) shows that the S atom is extruded from the molecule plane and becomes less affected by the rest parts of the molecule, and this might be considered as a preliminary theoretical explanation for the effect of hydrogenation on the adsorption structure of 4,6-DMDBT.

5. CONCLUSIONS

First principle periodic DFT calculations have been used to study the desulfurization of thiophene and its hydrogenated derivatives on Pt(111). The HDS network has been mapped out.

Thiophene has two types of adsorption structures (the parallel cross-bridge and partially tilted bridge-hollow configurations), whereas for its hydrogenated derivatives, the molecule gradually lifts up from the surface with the addition of hydrogen atoms. In all the adsorbed thiophenic compounds, the S atom is always sp³-hybridized; the C atom in the methylene group is always sp³-hybridized, whereas in the methyne group, it is either sp²- or sp³-hybridized, depending on how the group interacts with the surface Pt atoms. On the basis of the thermodynamic and kinetic analysis of the elementary steps, the DDS pathway is proposed for thiophene on Pt(111), and hydrogenations of thiophene do not reduce energy barriers for the C–S bond cleavage. The platinum catalyst exhibits high desulfurization efficiency via the DDS pathway for simple S-containing compounds, but for the more complicated molecules, such as 4,6-DMDBT, the isomerization caused by hydrogenation process might be important for S removal.

■ ASSOCIATED CONTENT

S Supporting Information. PESs for desulfurization of bridge-fcc adsorbed thiophene, conversion between different adsorption configurations of thiophene, and hydrogenation of cross-bridge adsorbed thiophene and the C₄H₄S(thiolate)-A intermediate. C–S bond lengths of intermediates involved in the desulfurization reactions. This information is available free of charge via the Internet at <http://pubs.acs.org/>.

■ AUTHOR INFORMATION

Corresponding Author

*Phone: 86-532-8698-1334. Fax: 86-532-8698-3363. E-mail: (W.G.) wgyuo@upc.edu.cn, (H.S.) shanh@upc.edu.cn.

■ ACKNOWLEDGMENT

This work was supported by the Program for Changjiang Scholars and Innovative Research Team in University (IRT0759) of MOE, PRC, NSFC (10979077 and 21003158); State Key Basic Research Program of China (2006CB202505); CNPC Science & Technology Innovation Foundation (2009D-5006-04-07); the Fundamental Research Funds for the Central Universities (09CX05002A); and the Graduate Innovative Foundation of China University of Petroleum (CXYB11-11).

■ REFERENCES

- (1) Weigand, B. C.; Friend, C. M. *Chem. Rev.* **1992**, *92*, 491.
- (2) Friend, C. M.; Chen, D. A. *Polyhedron* **1997**, *16*, 3165.
- (3) Yang, R. T.; Hernández-Maldonado, A. J.; Yang, F. H. *Science* **2003**, *301*, 79.
- (4) Topsøe, H.; Clausen, B. S.; Massoth, F. E. *Hydrotreating Catalysis, Science and Technology*; Springer: Berlin, 1996; Vol. 11.
- (5) Todorova, T.; Prins, R.; Weber, T. J. *Catal.* **2007**, *246*, 109.
- (6) Krebs, E.; Silvi, B.; Daudin, A.; Raybaud, P. *J. Catal.* **2008**, *260*, 276.
- (7) Prins, R. In *Handbook of Heterogeneous Catalysis*, 2nd ed.; Ertl, G., Knözinger, H., Schüth, F., Weitkamp, J., Eds.; Wiley-VCH: Weinheim, 2008; Vol. 6.
- (8) Bianchini, C.; Meli, A. *Acc. Chem. Res.* **1998**, *31*, 109.
- (9) Sugioka, M.; Sado, F.; Kurosaka, T.; Wang, X. *Catal. Today* **1998**, *45*, 327.
- (10) Sugioka, M.; Andalaluna, L.; Morishita, S.; Kurosaka, T. *Catal. Today* **1997**, *39*, 61.

- (11) Sun, Y. Y.; Wang, H. M.; Prins, R. *Catal. Today* **2010**, *150*, 213.
- (12) Whitehurst, D. D.; Isoda, T.; Mochida, I. *Adv. Catal.* **1998**, *42*, 345.
- (13) Raybaud, P. *Appl. Catal., A* **2007**, *322*, 76.
- (14) Paul, J. F.; Cristol, S.; Payen, E. *Catal. Today* **2008**, *130*, 139.
- (15) Moses, P. G.; Hinnemann, B.; Topsøe, H.; Nørskov, J. K. *J. Catal.* **2007**, *248*, 188.
- (16) Moses, P. G.; Hinnemann, B.; Topsøe, H.; Nørskov, J. K. *J. Catal.* **2009**, *268*, 201.
- (17) Lauritsen, J. V.; Nyberg, M.; Nørskov, J. K.; Clausen, B. S.; Topsøe, H.; Lægsgaard, E.; Besenbacher, F. *J. Catal.* **2004**, *224*, 94.
- (18) Niquille-Röthlisberger, A.; Prins, R. *J. Catal.* **2006**, *242*, 207.
- (19) Yoshimura, Y.; Toba, M.; Matsui, T.; Harada, M.; Ichihashi, Y.; Bando, K. *Appl. Catal., A* **2007**, *322*, 152.
- (20) Niquille-Röthlisberger, A.; Prins, R. *Catal. Today* **2007**, *123*, 198.
- (21) Gate, B. C. *Catalytic Chemistry*; Wiley: New York, 1992.
- (22) Zaera, F.; Kollin, E. B.; Gland, J. L. *Surf. Sci.* **1987**, *184*, 75.
- (23) Roberts, J. T.; Friend, C. M. *Surf. Sci.* **1987**, *186*, 201.
- (24) Kelly, D. G.; Odriozola, J. A.; Somorjai, G. A. *J. Phys. Chem.* **1987**, *91*, 5695.
- (25) Cocco, R. A.; Tatarchuk, B. J. *Surf. Sci.* **1989**, *218*, 127.
- (26) Stohr, J.; Gland, J. L.; Kollin, E. B.; Koestner, R. J.; Johnson, A. L.; Muetterties, E. L.; Sette, F. *Phys. Rev. Lett.* **1984**, *53*, 2161.
- (27) Lang, J. F.; Masel, R. I. *Surf. Sci.* **1987**, *183*, 44.
- (28) Gentle, T. M. *Energy Res. Abstr.* **1984**, *9*, 28229.
- (29) Netzer, F. P.; Bertel, E.; Goldmann, A. *Surf. Sci.* **1988**, *201*, 257.
- (30) Delley, B. *J. Chem. Phys.* **1990**, *92*, 508.
- (31) Delley, B. *J. Phys. Chem.* **1996**, *100*, 6107.
- (32) Delley, B. *J. Chem. Phys.* **2000**, *113*, 7756.
- (33) Perdew, J. P.; Wang, Y. *Phys. Rev. B* **1986**, *33*, 8800.
- (34) Perdew, J. P.; Wang, Y. *Phys. Rev. B* **1992**, *45*, 13244.
- (35) Popa, C.; Offmians, W. K.; Santen, R. A. V.; Jansen, A. P. J. *Phys. Rev. B* **2006**, *74*, 155428.
- (36) Monkhorst, H. J.; Pack, J. D. *Phys. Rev. B* **1976**, *13*, 5188.
- (37) Hayek, K.; Glassl, H.; Gutmann, A.; Leonhard, H.; Prutton, M.; Tear, S. P.; Welton-Cook, M. R. *Surf. Sci.* **1985**, *152*, 419.
- (38) Lin, X.; Ramer, N. J.; Rappe, A. M.; Hass, K. C.; Schneider, W. F.; Trout, B. L. *J. Phys. Chem. B* **2001**, *105*, 7739.
- (39) Yang, Z.; Wu, R.; Rodriguez, J. A. *Phys. Rev. B: Condens. Matter* **2002**, *65*, 155409.
- (40) Herzberg, G. *Electronic Spectra and Electronic Structure of Polyatomic Molecules*; Van Nostrand: New York, 1966.
- (41) Halgren, T. A.; Lipscomb, W. N. *Chem. Phys. Lett.* **1977**, *49*, 225.
- (42) Mittendorfer, F.; Hafner, J. *Surf. Sci.* **2001**, *492*, 27.
- (43) Morin, C.; Eichler, A.; Hirschl, R.; Sautet, P.; Hafner, J. *Surf. Sci.* **2003**, *540*, 474.
- (44) Blyth, R. I. R.; Mittendorfer, F.; Hafner, J.; Sardar, S. A.; Duschek, R.; Netzer, F. P.; Ramsey, M. G. *J. Chem. Phys.* **2001**, *114*, 935.
- (45) Orita, H.; Itoh, N. *Surf. Sci.* **2004**, *550*, 177.
- (46) Stohr, J.; Kollin, E. B.; Fischer, D. A.; Hastings, J. B.; Zaera, F.; Sette, F. *Phys. Rev. Lett.* **1985**, *55*, 1486.
- (47) Ohta, T. *Physica B (Amsterdam)* **1995**, *208–209*, 427.
- (48) Imanishi, A.; Yagi, S.; Yokoyama, T.; Kitajima, Y.; Ohta, T. *J. Electron Spectrosc. Relat. Phenom.* **1996**, *80*, 151.
- (49) Terada, S.; Yokoyama, T.; Sakano, M.; Imanishi, A.; Kitajima, Y.; Kiguchi, M.; Okamoto, Y.; Ohta, T. *Surf. Sci.* **1998**, *414*, 107.
- (50) Sexton, B. A. *Surf. Sci.* **1985**, *163*, 99.
- (51) Joshi, Y. V.; Ghosh, P.; Venkataraman, P. S.; Delgass, W. N.; Thomson, K. T. *J. Phys. Chem. C* **2009**, *113*, 9698.
- (52) Angelici, R. J. *Acc. Chem. Res.* **1988**, *21*, 387.
- (53) Yao, X. Q.; Li, Y. W.; Jiao, H. J. *J. Mol. Struct.: THEOCHEM* **2005**, *726*, 81.
- (54) Chen, J.; Daniels, L. M.; Angelici, R. J. *J. Am. Chem. Soc.* **1991**, *113*, 2544.
- (55) Zhu, H. Y.; Guo, W. Y.; Jiang, R. B.; Zhao, L. M.; Lu, X. Q.; Li, M.; Fu, D. L.; Shan, H. H. *Langmuir* **2010**, *26*, 12017.
- (56) Michaelides, A.; Hu, P. *J. Chem. Phys.* **2001**, *115*, 8570.
- (57) Saeys, M.; Reyniers, M. F.; Marin, G. B.; Neurock, M. *J. Phys. Chem. B* **2002**, *106*, 7489.
- (58) Morin, C.; Simon, D.; Sautet, P. *J. Phys. Chem. B* **2003**, *107*, 2995.
- (59) Joshi, Y. V.; Ghosh, P.; Venkataraman, P. S.; Delgass, W. N.; Thomson, K. T. *J. Phys. Chem. C* **2009**, *113*, 9698.
- (60) Mittendorfer, F.; Hafner, J. *J. Catal.* **2003**, *214*, 234.
- (61) Rodriguez, J. A. *Surf. Sci.* **1992**, *278*, 326.
- (62) Rodriguez, J. A. *J. Phys. Chem. B* **1997**, *101*, 7524.
- (63) Niquille-Röthlisberger, A.; Prins, R. *J. Catal.* **2005**, *235*, 229.